Electronic Supplementary Information

Stabilization of a Nanoporous NiCu Dilute Alloy Catalyst for Non-oxidative Ethanol Dehydrogenation

Nare Janvelyan, Matthijs A. van Spronsen, Cheng Hao Wu, Zhen Qi, Matthew M. Montemore, Junjun Shan, Dmitri N. Zakharov, Fang Xu, J. Anibal Boscoboinik, Miquel B. Salmeron, Eric A. Stach, Maria Flyztani-Stephanopoulos, Juergen Biener, and Cynthia M. Friend*
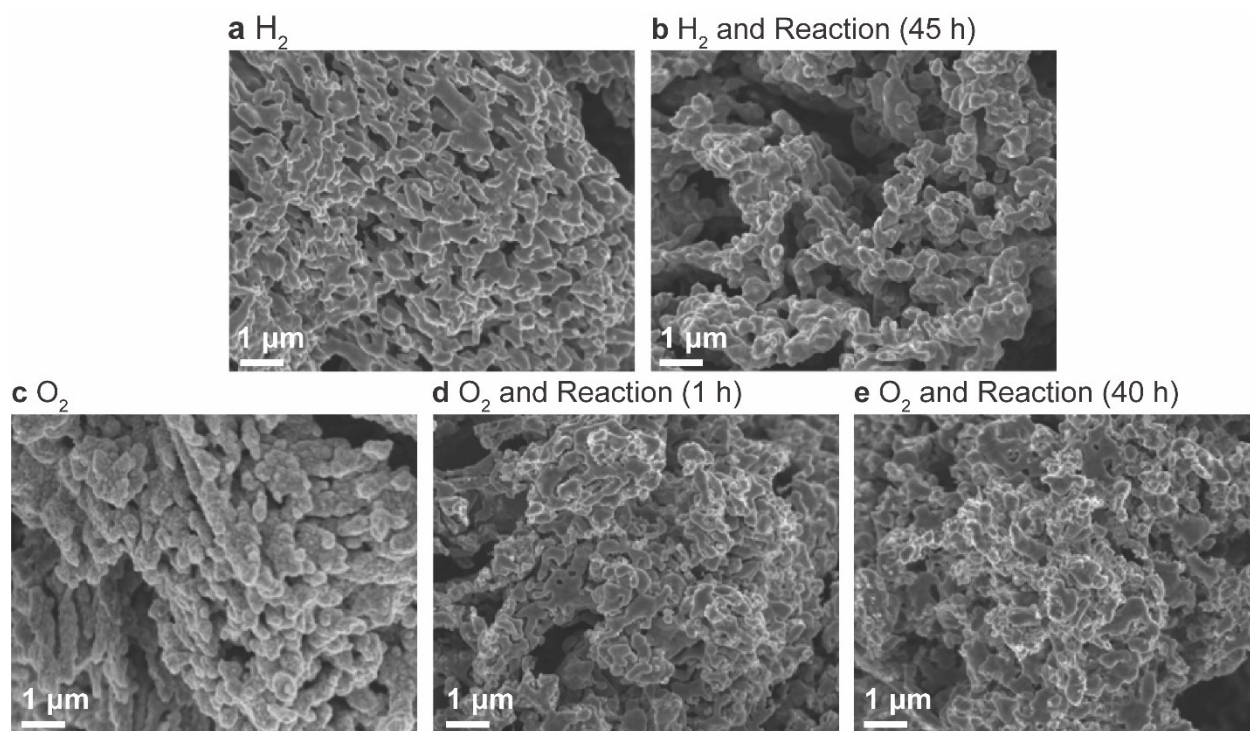
Figure S1. a) The initially smooth ligament surface morphology of nanoporous NiCu (np NiCu) after H_2 pretreatment at 350 °C and exposure to ethanol for 45 h (b) roughens after O_2 exposure at 250 °C (c) while subsequent ethanol exposure at 250 °C restores the original smooth morphology (d,e).
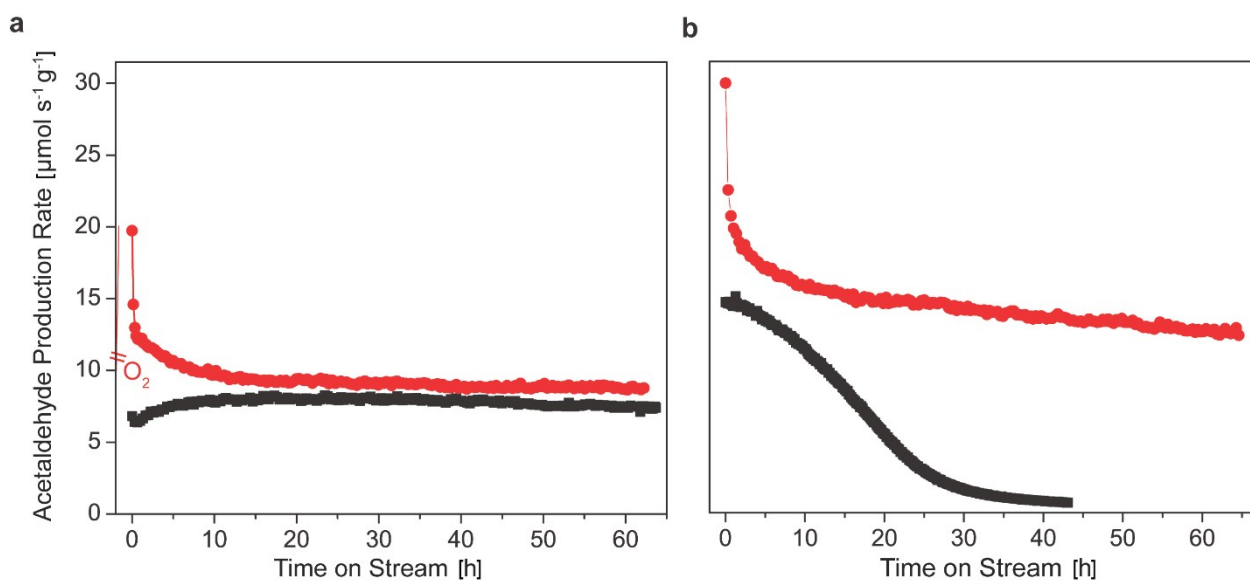
Figure S2. a) Nanoporous Cu (np Cu) stably produces acetaldehyde up to 60 h regardless of pretreatment (H_2, black & O_2, red). b) Np NiCu quickly deactivates after H_2 pretreatment (black) while it maintains a higher activity than np Cu after O_2 pretreatment even after 60 h on stream (red).

S1 AP-XPS Sample Loading

Both the outer surface and the cross section of np NiCu were investigated by breaking the monolithic sample (12 mm × 3 mm × 1 mm) into two pieces. One of these pieces was mounted on the sample holder with the cross section facing the X-ray beam (left, Figure S3a) while the other was mounted with its outer surface facing the X-ray beam (right, Figure S3a). Both pieces were held onto a Ta back-plate with Ta strips spot welded on each side. This construction was then loaded on a Pt button heater and mounted within the AP-XPS chamber. The catalytic performance was monitored using a capillary aimed at the sample surface connected to a mass spectrometer located in a separate chamber.
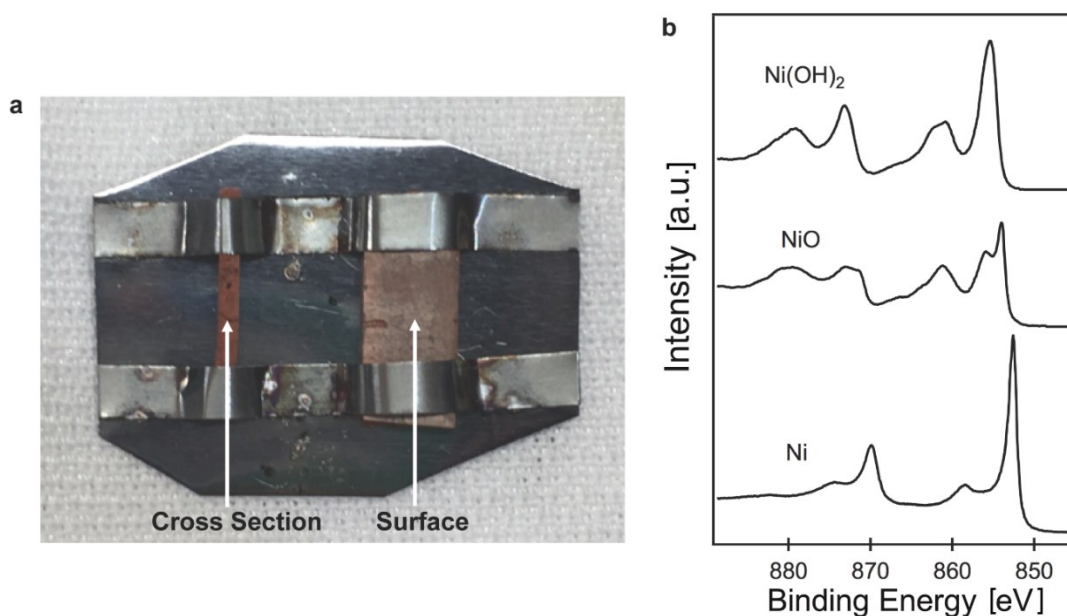

Figure S3. a) AP-XPS np NiCu cross section (left) and outer surface (right) samples on Ta back-plate with Ta strips running across the top and bottom affixing the samples. Linear combinations of the literature[1] Ni 2p reference spectra shown in b) were used to fit the measured AP-XPS.

2

S2 Spectral Analysis

All spectra were fit using Voigt line-shapes after subtracting a Shirley background[2] to obtain individual spectral features. Due to their complicated line-shapes, Ni 2p spectra were analyzed using least-square fitting based on a linear combination of area-normalized reference $2p_{3/2}$ spectra of Ni^0, Ni^{2+}, and $Ni(OH)_2$ to extract the percentage of each species present. Reference spectra were obtained from the literature using the online program WebPlotDigitizer (Figure S3b)[1]. Because the Cu 2p spectra exhibited either pure Cu^{2+} or a mixture of Cu^0 and Cu^{+1}, which are difficult to distinguish by XPS, no further fitting was conducted. Efforts to fit the Zn 2p spectra were not made as the Zn metal and oxide components overlap and thus quantification is difficult for mixtures[3]. Atomic ratios were calculated using peak area (PA), ionization cross-sections (ICS) of each element[4], and the photon flux (PF) at the corresponding photon energy using the following formula:

$$Ratio\,A/B = \frac{PA(A)}{PA(B)} \times \frac{ICS(B)}{ICS(A)} \times \frac{PF@E_{hv,B}}{PF@E_{hv,A}}$$

Because most near-edge X-ray absorption fine structure (NEXAFS) spectra showed prominent Cu^0 characteristics, the energy calibration of NEXAFS spectra was conducted by aligning the Cu^0 peaks and corresponding satellites to reported literature values. To extract Cu^0/Cu^{1+} ratios, least-square fitting was performed based on the linear combination of Cu^0 and Cu^{1+} area-normalized reference spectra of the L_3 region.
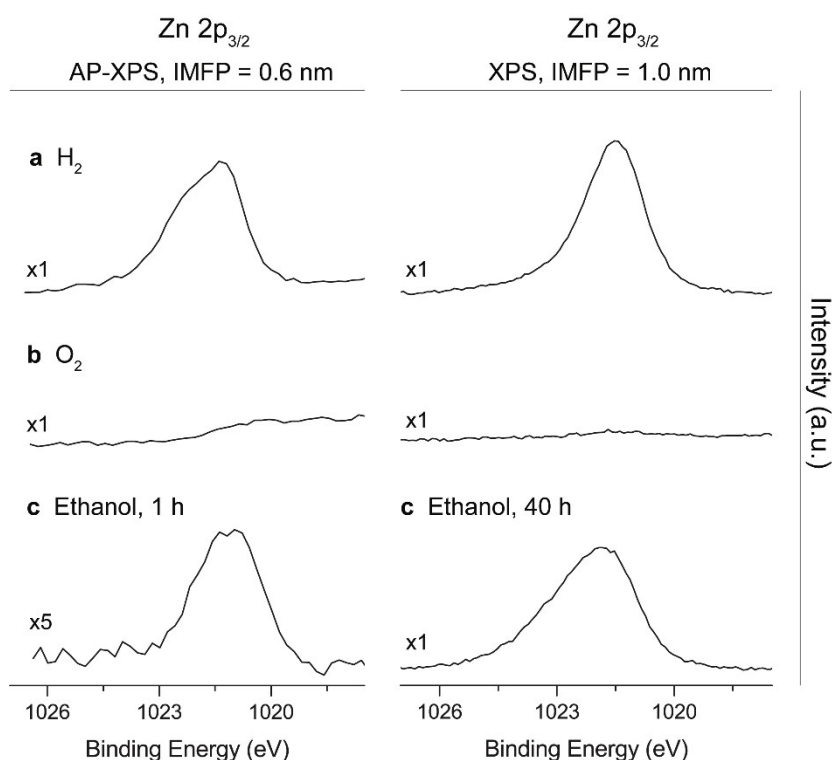

Figure S4. Corresponding AP-XPS (hv=1221 eV) and conventional XPS (hv=1487 eV) Zn $2p_{3/2}$ data to Figure 2: a) after H_2 pretreatment (AP-XPS: *in situ* at 350 °C, 1 Torr, 1 h; conventional XPS: *ex situ* at 10 vol.% H_2/He at 760 Torr, 1 h), b) after oxidation (AP-XPS: *in situ* at 250 °C, 1 Torr, 1 h; conventional XPS: *ex situ* at 20 vol.% H_2/He at 760 Torr, 1 h), and c) in ethanol (AP-XPS) or after 40-h of ethanol exposure (conventional XPS: 6 vol.% ethanol/He at 760 Torr, 250°C). Zn is no longer detected at the surface after oxidation due to the Cu oxide overlayer but becomes detectable again (although at lower concentrations) after subsequent reduction in ethanol. Because of the overlap of Zn and ZnO peaks, no efforts were made to fit the Zn 2p spectra. Spectra recorded under ultra-high vacuum (UHV) at room temperature (RT), except for AP-XPS spectrum after 1-h ethanol exposure (c, left), which was collected in 0.2 Torr ethanol at 250 °C.
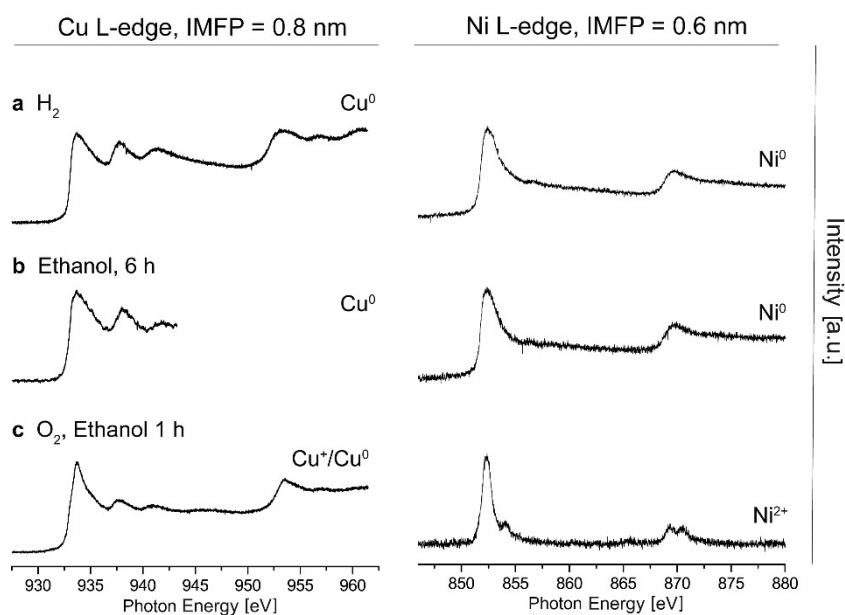
Cu L-edge, IMFP = 0.8 nm   Ni L-edge, IMFP = 0.6 nm

a H$_2$ Cu^0

    Ni^0

b Ethanol, 6 h

Cu^0

    Ni^0

c O$_2$, Ethanol 1 h

Cu$^+$/Cu^0

    Ni^{2+}

Intensity [a.u.]

930 935 940 945 950 955 960   850 855 860 865 870 875 880
Photon Energy [eV]   Photon Energy [eV]

Figure S5. NEXAFS data a) after *in situ* reduction with H$_2$ (350 °C, 1 Torr, 1 h), showing reduced Ni and Cu surface species; b) after ethanol exposure (250 °C, 0.2 Torr, 6 h) where Ni and Cu remain metallic; and c) after sequential oxidation (250 °C, 1 Torr O$_2$, 1 h) and exposure to ethanol (250 °C, 0.2 Torr, 1 h), showing that Cu is partially reduced to Cu^0 (71%) and Cu^{1+} (29%) while Ni remains mostly oxidized as Ni^{2+}. Spectra recorded at RT and under UHV, except for c (250 °C, 0.2 Torr ethanol)

i Cu 2p, IMFP = 1.3 nm   **ii** Ni 2p, IMFP = 1.2 nm

a UHV, RT   Cu^0/Cu^{1+}

    Ni^{2+}

Cu^{2+}

×25

×10

b H$_2$

Ni^0

Intensity [a.u.]

960 950 940 930   880 870 860 850
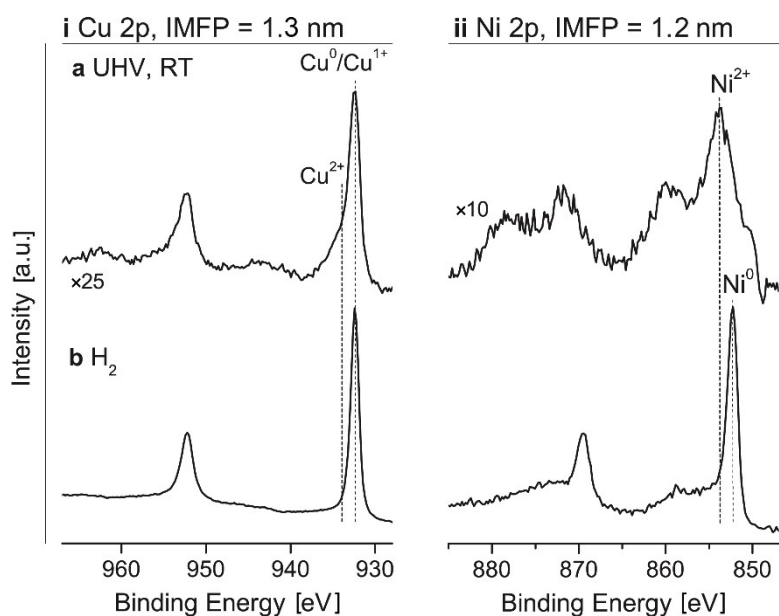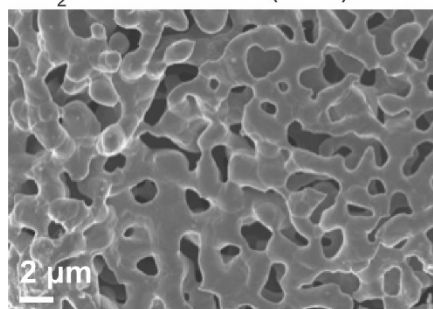Binding Energy [eV]   Binding Energy [eV]

Figure S6. AP-XPS measurements taken with a higher X-ray photon energy reveal that Cu and Ni are reduced in the subsurface region after *in situ* (350 °C, 1 Torr, 1 h) H$_2$ treatment. Both spectra recorded at RT and under UHV. Cu (Ni) spectra were taken with a photon energy of 1600 eV (1500 eV) corresponding to photoelectrons with a kinetic energy of 667 eV (647 eV).

4

Table S1. AP-XPS quantification (200 eV kinetic energy, inelastic mean free path (IMFP) of around 0.6 nm, units in at.%). The „As loaded" sample was *ex situ* H_2 pretreated in flow reactor: 10% H_2 in He at 760 Torr, 350 °C, 20 mL min^{-1} for 1 h. Spectra recorded at room temperature under ultra-high vacuum unless stated otherwise.

Condition	Surface			Cross Section		
	Cu	Ni	Zn	Cu	Ni	Zn
As loaded (*ex situ* H_2 treated)	83.0	5.6	11.4	89.0	3.0	5.6
In H_2 (350 °C, 1 Torr, 1 h)	65.0	12.7	22.3	85.8	3.8	10.4
After H_2 treatment	71.6	11.3	17.1	76.6	2.4	21.0
Post 6-h ethanol exposure (250 °C)	67.5	10.7	21.8	78.6	2.8	18.6
After O_2 treatment (250°C, 1 Torr, 1 h)	99.6	0.0	0.4	100.0	0.0	0.0
In ethanol (250°C, 0.2 Torr, 1 h)	89.8	5.2	5.0	99.1	No spec	0.9

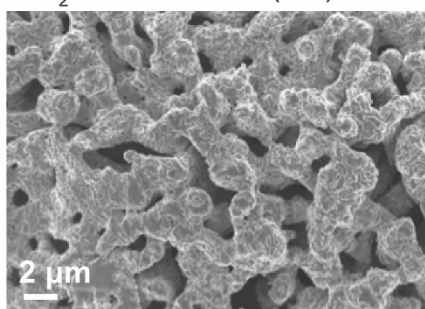**a** H_2 and Reaction (60 h)   **b** O_2 and Reaction (1 h)

Figure S7. Np NiCu with larger feature sizes a) after H_2 and exposure to reaction conditions for 60 h and b) after O_2 and exposure to reaction conditions for 1 h.
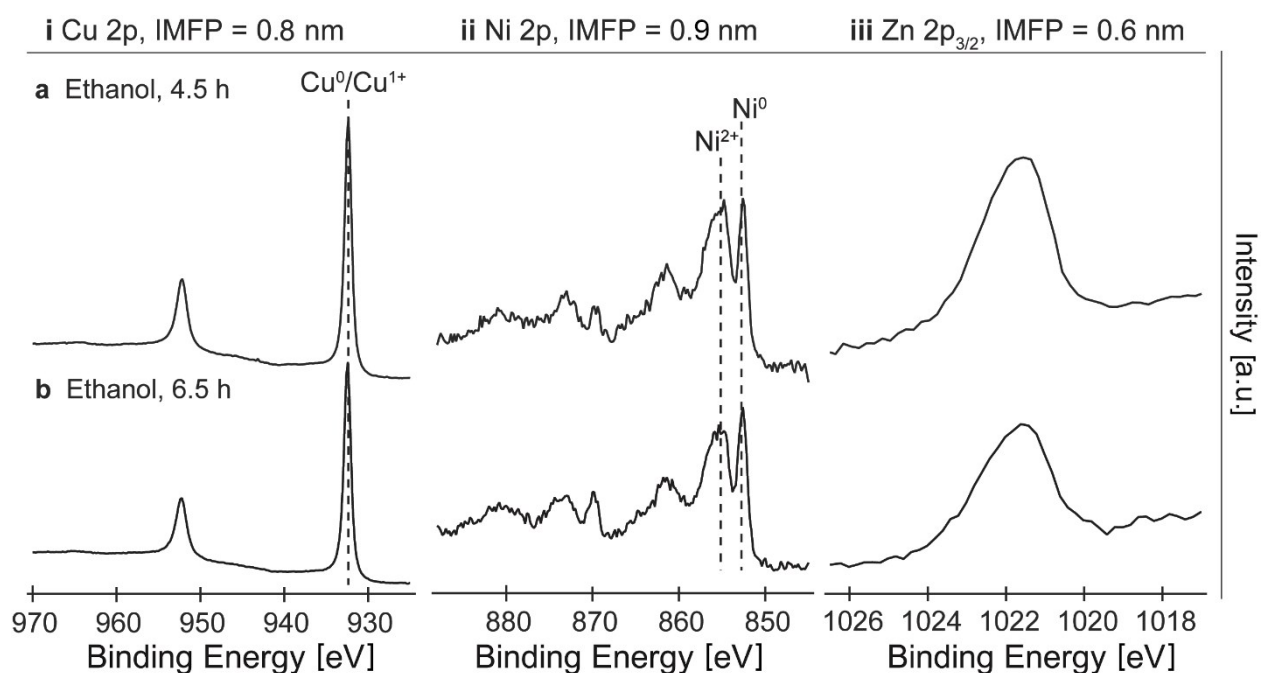
i Cu 2p, IMFP = 0.8 nm   ii Ni 2p, IMFP = 0.9 nm   iii Zn 2p$_{3/2}$, IMFP = 0.6 nm

a Ethanol, 4.5 h   Cu^0/Cu^{1+}

Ni^0

Ni^{2+}

b Ethanol, 6.5 h

Intensity [a.u.]

970 960 950 940 930
Binding Energy [eV]

880 870 860 850
Binding Energy [eV]

1026 1024 1022 1020 1018
Binding Energy [eV]

Figure S8. AP-XPS data after O_2 pretreatment and exposure to ethanol for 4.5 h and 6.5 h (250 °C, 0.2 Torr) revealing a Cu^0/Cu^{1+} mixture and mostly oxidized Ni at the surface. Compared to the spectra after 1 h of exposure to ethanol (Figure 2c), the Ni spectra after 4.5–6.5 h of exposure to ethanol have a clear contribution from Ni^0. The corresponding least-square fitting results of the Ni oxidation state are summarized in Table S2. The reduction rate of Ni oxide is initially very fast, slowing as the process is nucleation and limited by diffusion at these low temperatures[5]. An increase of ~6% Ni^0 over a 2 h period indicates the process has reached this regime. Other studies also reported that Ni oxide does not completely reduce in 6 h at 250 °C with ethanol or H$_2$[5-8]. Spectra collected with a 1221-eV photon energy, corresponding to IMFPs of 0.8 nm, 0.9 nm, and 0.6 nm for Cu, Ni, and Zn, respectively.

Table S2. Quantification of Ni oxidation states in AP-XPS (collected with a photon energy leading to a IMFP of 0.6 nm (0.9 nm for the last two entries).

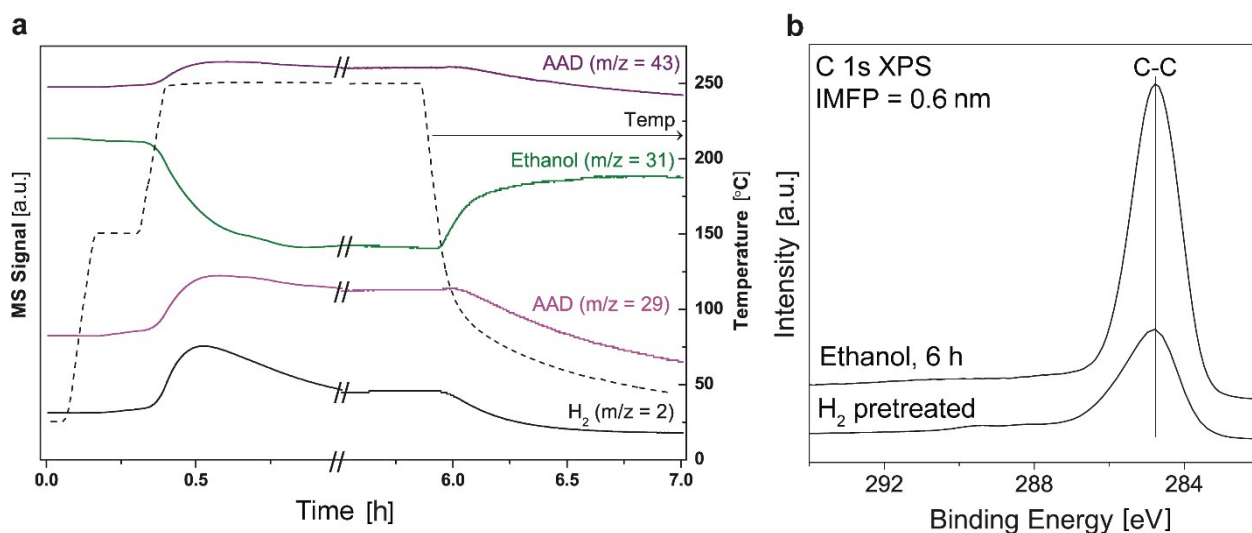| Surface	Ni^0 %	NiO %	Ni(OH) %
In H$_2$ (350°C, 1 Torr, 1 h)	100	0	0
After ethanol exposure (250°C, 0.2 Torr, 6 h)	100	0	0
After O$_2$ exposure (250°C, 1 Torr, 1 h)	No Ni on surface		
In ethanol (250°C, 0.2 Torr, 1 h)	19	36	45
In ethanol (250°C, 0.2 Torr, 4.5 h)	41	21	38
In ethanol (250°C, 0.2 Torr, 6.5 h)	47	15	38

Figure S9. a) Operando mass spectrometry (MS) during AP-XPS measurements of a H_2 pretreated np NiCu sample with varying temperature in 0.2 Torr ethanol showing stable production of acetaldehyde (AAD) and H_2 as co-product (not detected by GC-MS). The sample was held in 0.2 Torr ethanol at 250 °C for 6 h before decreasing the temperature. b) C 1s AP-XPS spectra (measured under UHV and at RT) of H_2-pretreated np NiCu measured as loaded and after exposure to ethanol (250 °C, 0.2 Torr, 6 h) revealing a substantial increase of carbon deposits (285 eV) at the outer surface of the np NiCu sample.

Table S3. Quantification of C accumulation in AP-XPS, plotted as the atomic ration of C/(Cu+Ni+Zn).

Condition	Surface	Cross Section
As loaded (*ex situ* H_2 treated)	1.4	0.5
After ethanol exposure (250°C, 0.2 Torr, 6 h)	10.3	3.2
After O_2 exposure (250°C, 1 Torr, 1 h)	0.2	0.2
In ethanol (250°C, 0.2 Torr, 1 h)	1.6	2.7
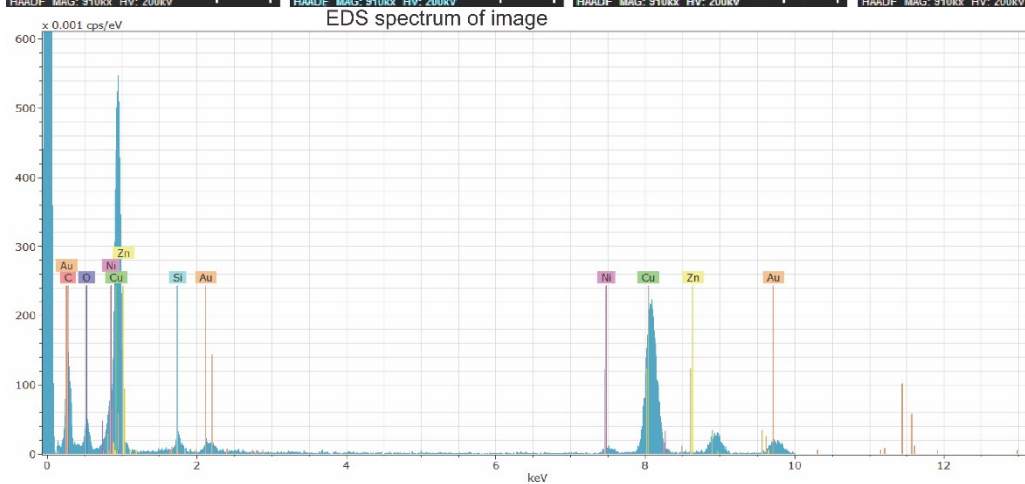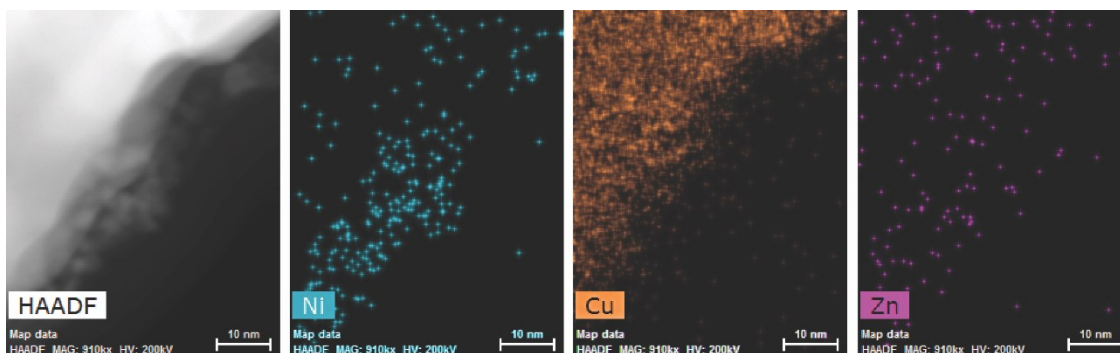
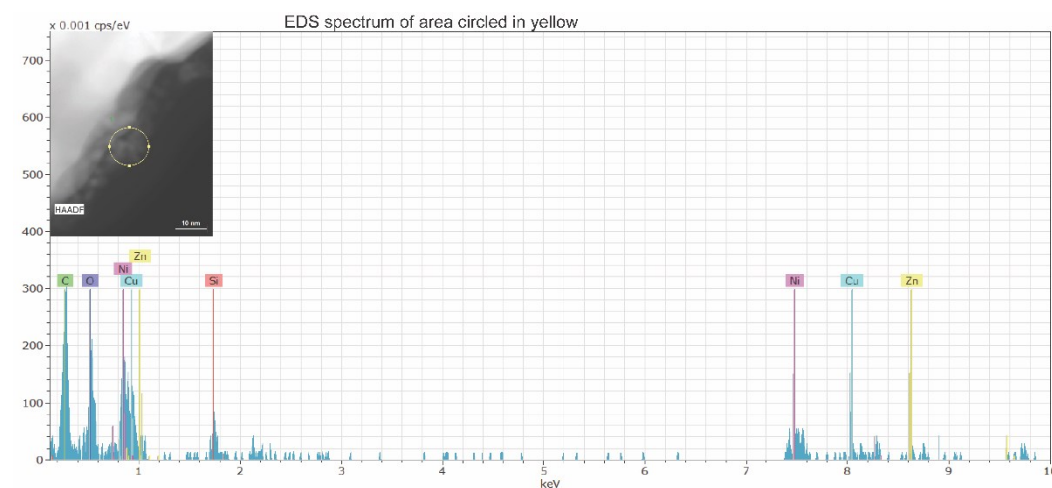| Quantification		Cu at.%	Ni at.%	Zn at.%
		93	5	2

Figure S10. *Ex situ* high-angle annular dark-field (HAADF) image (top left panel), individual elemental maps (top right 3 panels), and energy-dispersive X-ray spectroscopy (EDS) spectrum with quantification (middle panel) of np NiCu after O_2 treatment and exposure to ethanol (40 h) corresponding to Figure 3d. An EDS spectrum of the region where the particles sit on the surface (yellow circle) shows a Ni-rich area, although the signal-to-noise ratio is not very high. The Au and Si signals in the EDS spectra can be attributed to the transmission electron microscopy (TEM) grid and sample holder.
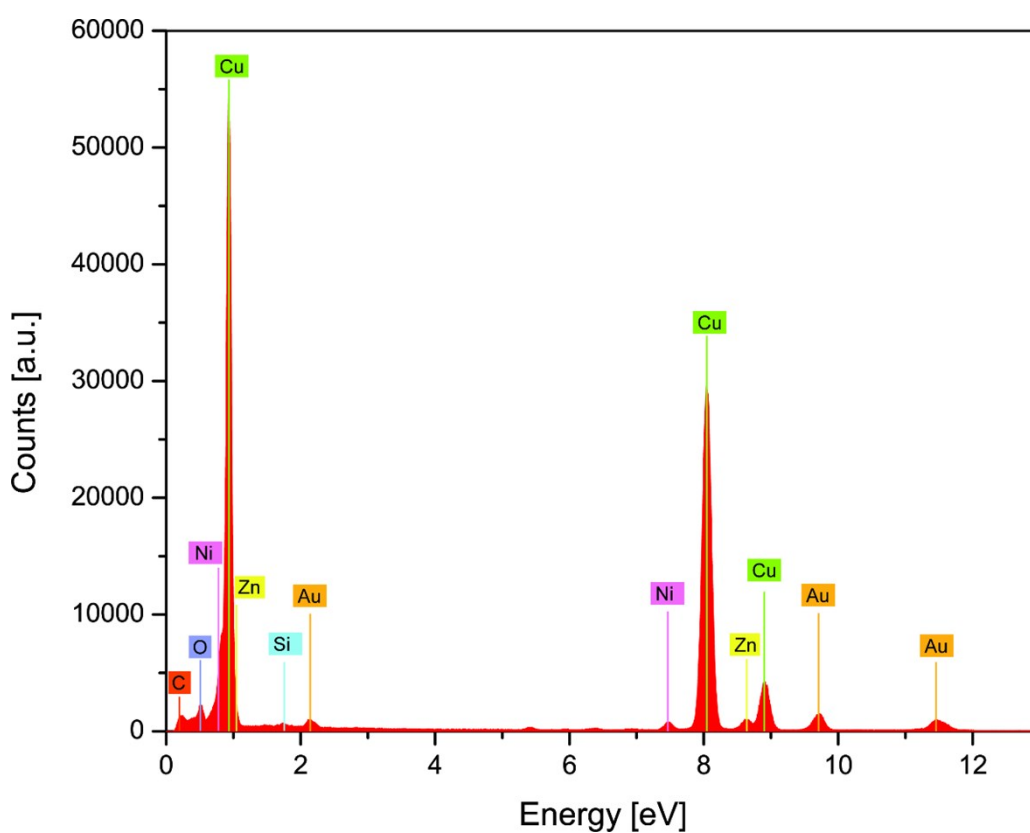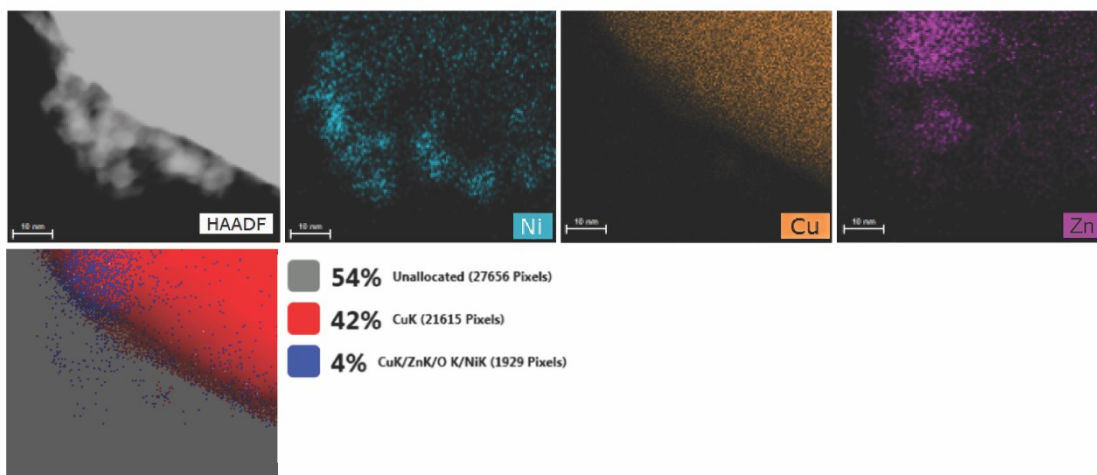
Phase in EDS map	Cu at.%	Ni at.%	Zn at.%
Unallocated (particle-containing region)	50	31	19
Cu K	97	1	2
Cu K/Zn K/O/Ni K	76	6	18
Whole Area (all phases)	74	13	13

Figure S11. *Ex situ* HAADF image and individual elemental maps of Ni, Cu, and Zn of deactivated np NiCu after H_2 treatment of active, O_2-treated np NiCu corresponding to Figure 3e. Phases identified by EDS analysis with corresponding EDS spectra and quantification. The unmarked Si (1.7 keV) and Au (2.1 keV and 9.7 keV) peaks in the EDS spectra are from the TEM grid and sample holder.

Table S4. Density functional theory calculations: surface energies of Ni atom or monolayer in first to third layers of Cu(110) or CuO(111). Lowest energies in bold.

Surface energies of Ni atom in Cu (110)			
O Coverage [ML]	**1st Layer [eV]**	**2nd Layer [eV]**	**3rd Layer [eV]**
0	0.44	0.05	**0.00**
0.167	0.08	**−0.05**	0.00
0.333	**−0.12**	−0.04	−0.02
1	**−0.60**	−0.02	0.07
CuO(111)	0.03	**−0.08**	0.00
H Coverage [ML]	**1st Layer [eV]**	**2nd Layer [eV]**	**3rd Layer [eV]**
0	0.44	0.05	**0.00**
0.167	0.15	**−0.16**	−0.02
0.333	0.03	**−0.18**	−0.04
1	**−0.65**	−0.18	0.02
Surface energies of Ni Monolayer in Cu (110)			
O Coverage [ML]	**1st Layer [eV/Ni atom]**	**2nd Layer [eV/Ni atom]**	**3rd Layer [eV/Ni atom]**
0	0.47	0.08	−0.01
1	−0.07	−0.05	0.07
CuO(111)	−0.09	−0.18	−0.04

References

1. A. P. Grosvenor, M. C. Biesinger, R. S. C. Smart and N. S. McIntyre, *Surf. Sci.*, 2006, **600**, 1771-1779.
2. D. A. Shirley, *Phys. Rev. B*, 1972, **5**, 4709-4714.
3. M. C. Biesinger, L. W. M. Lau, A. R. Gerson and R. S. C. Smart, *Appl. Surf. Sci.*, 2010, **257**, 887-898.
4. J. J. L. Yeh, I., *At. Data Nucl. Data Tables*, 1985, **33**, 1-155.
5. K. V. Manukyan, A. G. Avetisyan, C. E. Shuck, H. A. Chatilyan, S. Rouvimov, S. L. Kharatyan and A. S. Mukasyan, *J. Phys. Chem. C,* 2015, **119**, 16131-16138.
6. F. Coskun, S. Cetinkaya and S. Eroglu, *JOM*, 2017, **69**, 987-992.
7. Q. Jeangros, T. W. Hansen, J. B. Wagner, C. D. Damsgaard, R. E. Dunin-Borkowski, C. Hébert, J. Van herle and A. Hessler-Wyser, *J. Mater. Sci.*, 2013, **48**, 2893-2907.
8. J. A. Rodriguez, J. C. Hanson, A. I. Frenkel, J. Y. Kim and M. Pérez, *J. Am. Chem. Soc.*, 2002, **124**, 346-354.